applied sciences

MDPI

Article

Study on the Catalytic Decomposition Reaction of N_2O on MgO (100) in SO_2 and CO Environments

Xiaoying Hu [1,2,*], Erbo Zhang [1], Wenjun Li [1], Lingnan Wu [3], Yiyou Zhou [1], Hao Zhang [1] and Changqing Dong [1,2]

[1] National Engineering Laboratory for Biomass Power Generation Equipment, North China Electric Power University, Beijing 102206, China; zebhdkzs@163.com (E.Z.); lwjh2021@outlook.com (W.L.); zhouyiyouyiyou@163.com (Y.Z.); zhanghao03721102@163.com (H.Z.); cqdong@163.com (C.D.)
[2] State Key Laboratory of Alternate Electrical Power System with Renewable Energy Sources, North China Electric Power University, Beijing 102206, China
[3] Institute of Engineering Thermophysics, Chinese Academy of Sciences, Beijing 100190, China; wulingnan@126.com
* Correspondence: xiaoying_826@163.com; Tel.: +86-10-61772457

Abstract: To study the role of MgO in the reduction of N_2O in circulating fluidized bed boilers, density functional theory was used to evaluate heterogeneous decomposition. The interference of SO_2 and CO on N_2O was considered. N_2O on MgO (100) is a two-step process that includes O transfer and surface recovery processes. The O transfer process is the rate-determining step with barrier energy of 1.601 eV, while for the Langmuir–Hinshelwood and Eley–Rideal surface recovery mechanisms, the barrier energies are 0.840 eV and 1.502 eV, respectively. SO_2 has a stronger interaction with the surface-active O site than that of N_2O. SO_2 will occupy the active site and hinder N_2O decomposition. CO cannot improve the catalysis of MgO (100) for N_2O because O transfer is the rate-determining step. Compared with homogeneous reduction by CO, MgO has a limited catalytic effect on N_2O, where the barrier energy decreases from 1.691 eV to 1.601 eV.

Keywords: MgO (100); N_2O; density functional theory; SO_2; CO

Citation: Hu, X.; Zhang, E.; Li, W.; Wu, L.; Zhou, Y.; Zhang, H.; Dong, C. Study on the Catalytic Decomposition Reaction of N_2O on MgO (100) in SO_2 and CO Environments. *Appl. Sci.* **2022**, *12*, 5034. https://doi.org/10.3390/app12105034

Academic Editor: Raffaele Marotta

Received: 17 March 2022
Accepted: 12 May 2022
Published: 16 May 2022

1. Introduction

With the growing awareness of environmental protection, increasing attention has been paid to energy saving and emission reduction in the coal-fired power generation industry. China's newly issued air pollutant emission standards for thermal power plants [1] put forward strict requirements for nitrogen oxide emissions from coal-fired power plants. Compared with conventional pulverized coal boilers, circulating fluidized bed (CFB) boilers emit more N_2O. Under partial load conditions, the emission concentration of CFB boilers can reach 360 mg/Nm^3 [2], which is approximately an order of magnitude higher than that of a conventional pulverized coal-fired boiler. N_2O is a powerful greenhouse gas, with a global warming potential 310 times that of carbon dioxide and 21 times that of methane [3]. Nowadays, N_2O has been regarded as a substance that causes the most serious damage to the ozone layer [4]. Therefore, reducing N_2O emissions from CFB boilers should be prioritized. In CFB boilers, dolomite is a kind of common desulfurizer. Dolomite is a compound salt of calcium carbonate and magnesium carbonate, wherein its main component is $CaMg(CO_3)_2$. According to the reaction conditions, dolomite decomposes via a two-step ((1) and (2)) or one-step mechanism (3) [5]:

$$CaMg(CO_3)_2 \rightarrow MgO + CO_2 + CaCO_3 \quad (1)$$

$$CaCO_3 \rightarrow CaO + CO_2 \quad (2)$$

$$CaMg(CO_3)_2 \rightarrow MgO + CaO + 2CO_2 \quad (3)$$

The formation of MgO, either by dolomite decomposition or pulverized coal combustion, affects N_2O emissions as it depends on the in-depth exploration of N_2O decomposition and reduction catalyzed by MgO, which can better control the desulfurization and denitrification in a CFB boiler and lay the foundation for the development of catalysts. The results calculated by density functional theory (DFT) have shown that the MgO (001) surface with oxygen vacancy has the highest catalytic activity for the adsorption and decomposition of N_2O [6]. Meanwhile, the first-principle calculation results show that the oxygen ions on the surface are the active sites for MgO catalyzing N_2O decomposition, and the theoretically calculated activation energy is 33 kcal/mol [7]. In addition, experiments and density functional theory calculations also confirmed that the decomposition mechanism of N_2O on the MgO surface mainly includes the oxygen atom transfer process and surface reduction process [8].

However, in the actual CFB boilers, other flue gas components, such as SO_2 and CO, also affect the decomposition of N_2O catalyzed by MgO. The reduction process of N_2O with CO or SO_2 on the surface of catalysts involves a two-stepwise reaction mechanism [9]:

$$N_2O \rightarrow O_{ads} + N_2 \quad (4)$$

$$CO + O_{ads} \rightarrow CO_2 \text{ or } SO_2 + O_{ads} \rightarrow SO_3 \quad (5)$$

First, the N_2O reduction reaction starts with the dissociative adsorption of N_2O on the surface of the catalyst, yielding the N-2 molecule and an activate d oxygen moiety (O_{ads}) adsorbed over the catalyst. Then, the O_{ads} moiety is eliminated by CO or SO_2 molecule [10]. The reduction reaction of N_2O and CO or SO_2 is embodied in the following aspects: the catalyst surface provides a reactive site for CO and N_2O and improves N_2O reduction, while CO significantly reduces the activation energy of N_2 desorption on the surface of catalysts [11]. N_2O is assisted to be decomposed into reactive oxygen atoms (O_{ads}) and N_2 molecules by adsorption of SO_2 molecules, and then SO_2 molecules are oxidized by O_{ads} [12]. However, there is no study on the reaction mechanism of the MgO catalyst surface for CO or SO_2 reduction of N_2O, and the catalytic mechanism of MgO is still unknown.

In this paper, the mechanism of N_2O decomposition on MgO was studied to understand the effects of CO and SO_2 on the catalytic decomposition of N_2O and to better reveal the mechanism of nitrogen oxide transformation in CFB boilers and clarify the effect of desulfurization on nitrogen oxide emissions, which will help to control the emissions of nitrogen oxide and sulfur oxide in CFB boilers. In the first part, the calculation method is discussed, and the second part shows the MgO (100) surface model and the decomposition mechanism of N_2O on the MgO (100) surface. At the same time, the competitive adsorption of SO_2 on the MgO (100) surface and the effect of CO on the catalytic decomposition of N_2O are taken into account.

2. Materials and Methods

All the calculations were performed using a DFT based on quantum chemistry, which is realized by the DMol^3 [13,14] package of Materials Studio software. The generalized gradient approximation (GGA) and Perdew-Burke-Ernzerhof (PBE) basis set [15] are used to evaluate the exchange–correlation energy, while atomic base functions are expanded using double numerical base group plus polarization functions (DNP). In the calculation process, all the valence electrons are considered, and the inner electrons are not specially treated. The basis set superposition error (BSSE) of the Dmol^3 package is better than that of the Gaussian 6-311+G (3 df, 2 pd) basis set [16], as it can also provide a better description of the weaker keys. In addition, the processing method of using the GGA electronic development method with PBE for exchange–correlation potential has been widely used [8,17–19], and its computational accuracy can be compared with that of Gaussian 6-31G**. This calculation uses an atomic truncation radius of 4.8 Å and a Smalling value of 0.005 Ha to accelerate convergence. The convergence thresholds for energy, stress, and displacement herein are

2×10^{-5} Ha, 0.004 Ha/Å, and 0.005 Å, respectively. The Monkhorst–Pack k-point [20] sampling points of $3 \times 3 \times 3$ are used in the structural optimization of the MgO crystals, while the sampling points of $3 \times 3 \times 1$ are used in the energy calculation, structural optimization, and transition state search. The linear/quadratic synchronous transition (LST/QST) method [21] is used to identify the transition state of the reaction and optimize the transition state structure to ensure that the virtual frequency of the transition state is unique.

The adsorption energy E_{ad} of gas molecules on the surface is calculated as follows:

$$E_{ad} = E_{sys} - E_{ads} - E_{sur} \quad (6)$$

where E_{sys} is the total energy of the system after the gas molecules are adsorbed on the surface, E_{ads} is the energy of the adsorbed gas, and E_{sur} is the energy of the surface.

3. Results

3.1. MgO Surface Model

MgO belongs to a cubic crystal system with a space group number of *Fm3m* (225), meaning it has a sodium chloride crystal structure. To verify the rationality of the calculation method and accuracy, the structure of the crystal cell was optimized when studying the crystal. The lattice constant after structure optimization was 4.26 Å. In order to study the catalytic decomposition and catalytic reduction of N_2O by MgO, it was necessary to establish a reasonable surface model to characterize the surface properties of MgO. Surface energy is a measure of the breaking of chemical bonds between molecules during surface formation, and density functional theory (DFT) is a theoretical calculation based on the principles of quantum physics, which is very suitable for measuring surface energy [22]. Therefore, we first studied the energy of different MgO surfaces to determine the stable surface of MgO and compared the surface energies of two low-index MgO surfaces (100, 110). These two surfaces are plate models of 3–7 layers of MgO (100) and MgO (110) in the optimized MgO crystal, wherein each layer contains 8 Mg ions and 8 O ions. To avoid mutual interference between the mirror surfaces, a 12 Å vacuum layer was constructed perpendicular to the surface, and the surface energies of each surface were calculated as follows [23]:

$$\sigma_{surf} = \frac{(E_{slab} - NE_{bulk})}{2A_{surf}} \quad (7)$$

where σ_{surf} is the surface energies of each surface, E_{slab} is the total energy required to build the surface, E_{bulk} is the energy of the MgO cell after structure optimization, N is the number of MgO cells in the surface model, and A_{surf} is the surface area of the MgO (100) surface.

The surface energy calculated from Equation (7) is shown in Figure 1. It is clear that the surface energy of the MgO (100) surface is lower than that of the MgO (110) surface for the 3–7 layers of MgO (100) and MgO (110) models, indicating that the MgO (100) surface is more stable than the MgO (110) surface. Further, for alkaline earth metal oxides, the MgO (100) surface is more stable and compact than MgO (110) surface. These results are consistent with the results of Broqvist et al. [23]. When the number of surface layers gradually increases from three to seven, the surface energy of the MgO (100) surface changes by 1%. Considering the calculation and its accuracy, the MgO (100) five-layer surface model was used in subsequent calculations to study the performance of MgO catalytic decomposition and catalytic reduction of N_2O.

The constructed five-layer MgO (100) model is shown in Figure 2, wherein it can be seen that the highest occupied molecular orbital (HOMO) on the MgO (100) surface is mainly attributed to the oxygen sites of the edge mode, which indicates that the oxygen sites on the surface are more likely to participate in the catalytic reaction process of the surface than the magnesium sites on the surface. As shown in Figure 2c, the results of the partial density analysis (PDOS), the price band of the MgO (100) model is mainly contributed to by the 2p orbital of the surface oxygen ions, mainly distributed between the

−5 eV and Fermi energy levels. These results are in good agreement with the results of Broqvist et al. [23], who used the CASTEP module based on plane wave expansion.

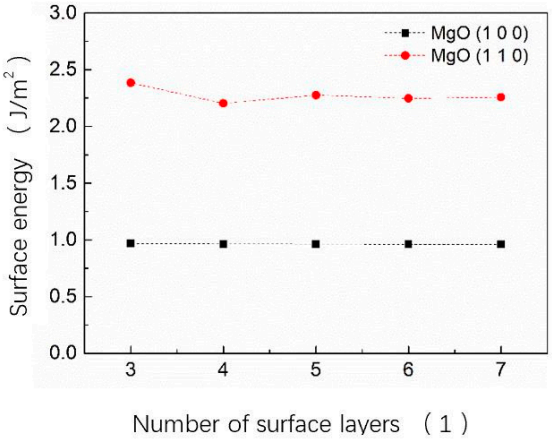

Figure 1. Surface energy of MgO (100) and MgO (110) surface models with different layers.

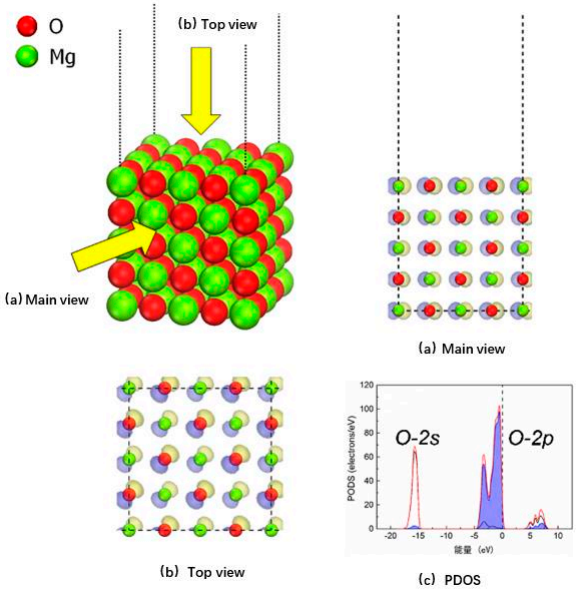

Figure 2. Surface model and state density analysis of MgO (100).

3.2. The Stable Adsorption Structure of N_2O on the Surface of MgO (100)

Adsorption is the first step in N_2O molecules' decomposition on the surface of MgO (100). The surface of MgO (100) consists of two active points of five-bit oxygen ions and five-bit magnesium ions. The calculation considers the eight adsorption structures of N_2O with its oxygen and external nitrogen ends perpendicular to the surface, the magnesium bit, the bridge level, and the empty position. The stable adsorption structure after structural optimization is shown in Figure 3.

Table 1 illustrates the stable adsorption structure, adsorption energy, and charge transfer of N_2O at different sites on the MgO (100) surface. One can notice that the adsorption energies (Eads) of N_2O molecules on the pristine MgO (100) were in the range of −0.011 to −0.092 eV. Thus, there is no obvious chemical adsorption when N_2O is adsorbed on the MgO (100) surface when considering the eight adsorption configurations [24,25]. Regarding adsorption energy, the adsorption energy of N_2O is the largest at the bridge site of its O end on the surface, reaching only 0.092 eV. In addition, the closest distance between N_2O and the surface after adsorption is the N-terminal of the N_2O at the site of the magnesium ion on the surface, with a distance of 2.663 Å. The farthest distance between

N_2O and the surface after adsorption is the O vacancy on the surface, with a distance of 3.760 Å. Note that the bond lengths of the N–O bond and N–N bond of the N_2O molecule did not change significantly before and after adsorption. In addition, according to the Mulliken charge analysis, the charge transfers of all eight adsorption configurations were small, wherein the maximum charge transfer occurred when N_2O was adsorbed at the Mg site at the N end of N_2O. After adsorption, N_2O transferred 0.012 *e* to the surface of MgO (100). According to the comprehensive adsorption energy, stable aggregate structure after adsorption, and charge transfer, N_2O is in a state of physical adsorption when in this structure.

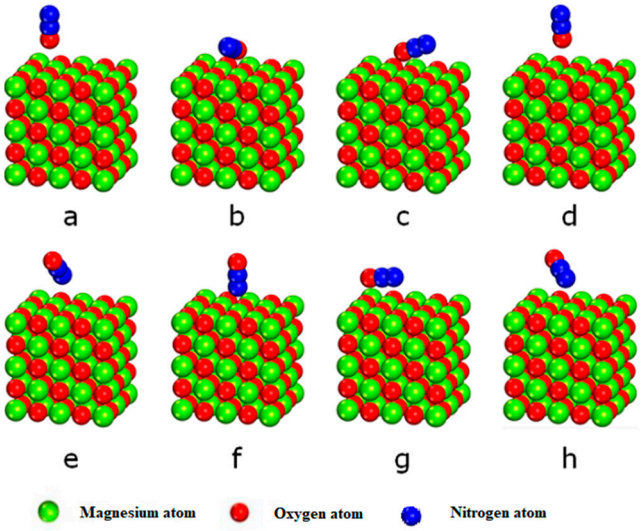

Figure 3. Stable adsorption structure of N_2O on MgO (100) surface. (**a**) The O is at O atop; (**b**) The O is at the top of the surface Mg; (**c**) The O is at the surface bridge; (**d**) O vacancy on the surface; (**e**) The N is at the top of the surface O; (**f**) The N is at the top of the surface Mg; (**g**) The N is at the surface bridge; (**h**) N vacancy on the surface.

Table 1. Adsorption energy, adsorption structure, and charge transfer of N_2O adsorption on MgO (100).

Serial Number	Adsorption Structure	E_{ad} eV	Nearest Distance Å	N–O Bond Length Å	N–N Bond Length Å	*q* *e*
a	The O is at O atop	−0.016	3.554	1.196	1.142	−0.004
b	The O is at the top of the surface Mg	−0.091	2.798	1.196	1.140	−0.002
c	The O is at the surface bridge	−0.092	2.800	1.197	1.140	0.002
d	O vacancy on the surface	−0.011	3.760	1.195	1.142	−0.005
e	The N is at the top of the surface O	−0.023	3.576	1.195	1.142	−0.004
f	The N is at the top of the surface Mg	−0.064	2.663	1.193	1.140	0.012
g	The N is at the surface bridge	−0.063	3.252	1.193	1.142	−0.007
h	N vacancy on the surface	−0.033	3.332	1.195	1.142	−0.005

3.3. Decomposition Path of N_2O on the Surface of MgO (100)

Decomposing N_2O on the MgO (100) surface first requires the transfer of N_2O oxygen atoms to the active site on the MgO (100) surface, as shown in Figure 4. This entire reaction must cross an energy barrier of 1.601 eV and simultaneously absorb 0.485 eV to form an ad-

sorbed atomic oxygen and N-N group. Note that the calculated results are close to the experimental (36 kcal/mol ≈ 1.561 eV) and theoretical values (33 kcal/mol ≈ 1.431 eV) obtained by Snis et al. [7], which are slightly higher than those obtained by Piskorz (31.8 kcal/mol ≈ 1.379 eV) and Karlsen et al. [26] (34.8 kcal/mol ≈ 1.509 eV). With regard to the surface catalytic activity of MgO (100), the energy barrier of the reaction is higher than 0.989 eV on the surface of CaO (100) and 1.228 eV on the surface of CaS (100). At low surface coverage, the catalytic activity of the surface is mainly determined by the difficulty of the transfer of oxygen atoms from N_2O to the surface-active site. Therefore, the catalytic activity of the oxygen transfer on the MgO (100) surface is lower than that of CaO, which is another commonly used desulfurized in furnaces that produce the desulfurization product CaS, creating a furnace reductive atmosphere. The activation energies of the oxygen atom transfer process on the surface of CaO (100) and CaS (100) are 0.989 eV and 1.228 eV, respectively [18].

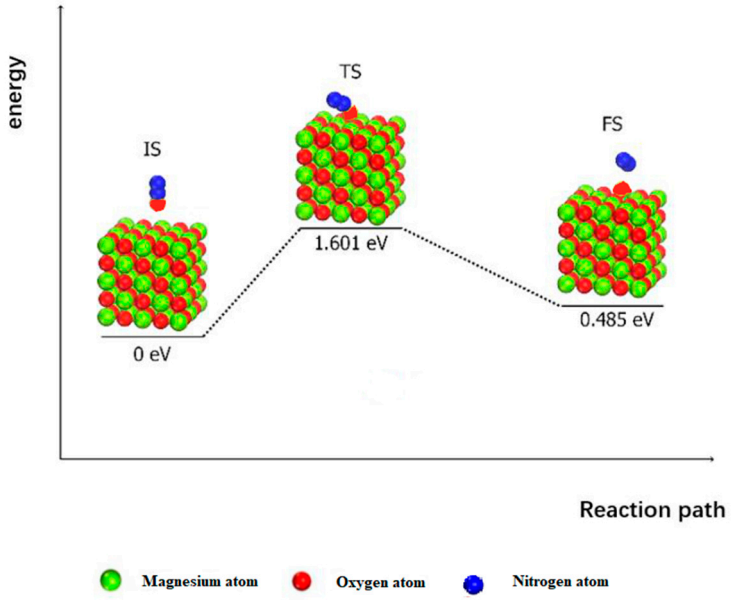

Figure 4. Oxygen atom transfer process of N_2O on MgO (100) surface.

At higher surface coverage, the activity of the MgO (100) surface to catalyze the decomposition of N_2O depends on the regeneration ability of the surface-active site, which is the ability to remove the active site and adsorb atomic oxygen. Figure 5 shows the energy diagram of the surface reduction of MgO (100) by the Langmuir–Hinshelwood (LH) mechanism, wherein two adsorbed oxygen atoms can be moved and reorganized to form an oxygen molecule, forming adsorbed oxygen on the surface of MgO (100). This reaction process must overcome an energy barrier of 0.840 eV and release 0.852 eV.

Another possible surface reduction process follows the Eley–Rideal (ER) mechanism, which is shown in Figure 6. Here, the adsorbed oxygen atom reacts with the subsequent N_2O molecules to form adsorbed oxygen and nitrogen molecules. This process needs to overcome 1.502 eV and release 0.419 eV.

Based on these results, the energy barrier of the surface reduction process of MgO (100) is lower than that of the oxygen atom transfer process at higher surface coverages. Therefore, the constant rate step of N_2O decomposition catalyzed by surface MgO (100) is the oxygen atom transfer process. Although the ability of the oxygen active site of the MgO (100) surface to catalyze N_2O decomposition is weaker than that of the CaO (100) and CaS (100) surfaces, its surface regeneration ability is better. Thus, in terms of N_2O decomposition catalyzed by MgO (100) surface, surface modification and the loading of active components are necessary to improve the surface catalytic activity for N_2O decomposition.

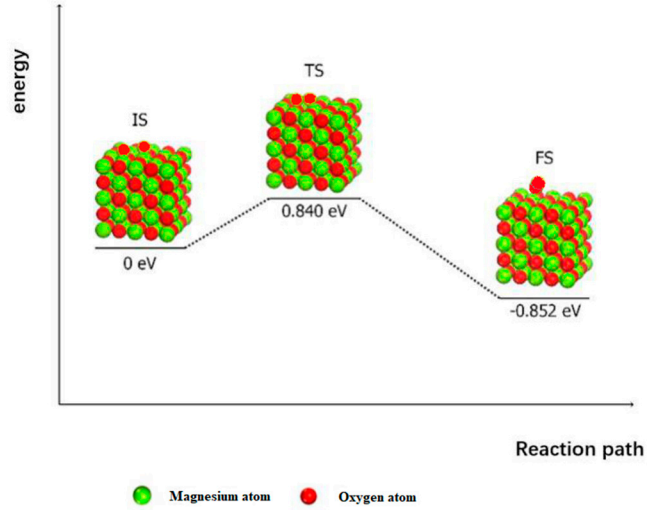

Figure 5. The surface reduction process of MgO (100) following the Langmuir–Hinshelwood (LH) mechanism.

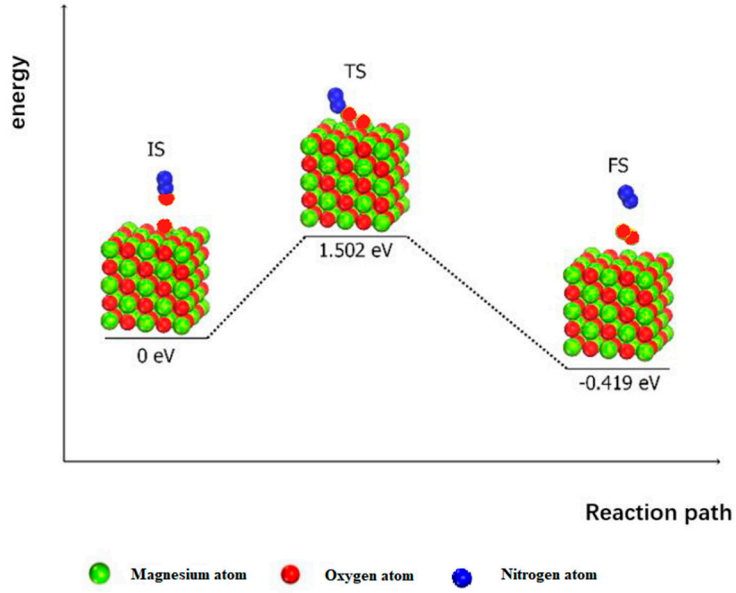

Figure 6. The surface reduction process of MgO (100) following the Eley–Rideal (ER) mechanism.

3.4. Effect of SO_2 and CO on the Decomposition of N_2O Catalyzed by MgO (100)

Other flue gas components in furnaces will affect the catalytic performance of N_2O decomposition on the surface of MgO (100). Thus, the adsorption of SO_2 on the MgO (100) surface was studied. The stable adsorption structure after geometric optimization is shown in Figure 7, and the adsorption energy, geometric structure, and Mulliken charge transfer after structure optimization are listed in Table 2.

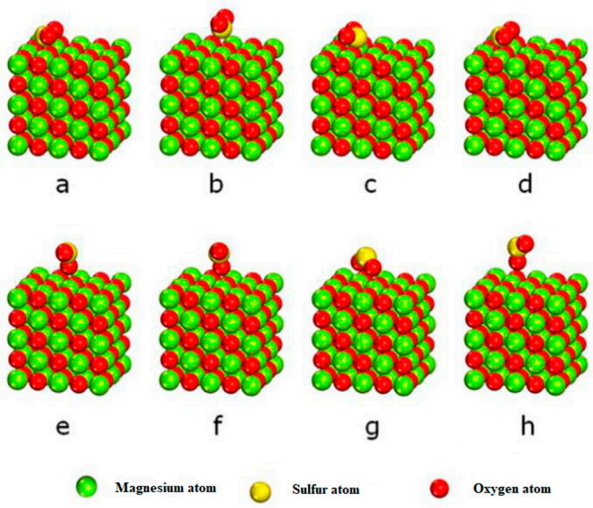

Figure 7. Stable adsorption structure of SO_2 molecules on the surface of MgO (100). (**a**) The S is at the top of the surface O; (**b**) The S is at the top of the surface Mg; (**c**) The S is at the surface bridge; (**d**) O vacancy on the surface; (**e**) The S is at the top of the surface O; (**f**) The S is at the top of the surface Mg; (**g**) The S is at the surface bridge; (**h**) S vacancy on the surface.

Table 2. Adsorption energy, adsorption structure, and charge transfer of SO_2 adsorption on the surface of MgO (100).

Serial Number	Adsorption Structure	E_{ad} eV	Nearest Distance Å	S–O Bond Length Å	S–O Bond Length Å	*q* *e*
a	The S is at the top of the surface O	−0.238	1.855	1.511	1.513	−0.440
b	The S is at the top of the surface Mg	−0.047	2.961	1.484	1.484	−0.077
c	The S is at the surface bridge	−0.239	1.837	1.510	1.514	−0.448
d	O vacancy on the surface	−0.239	1.837	1.510	1.514	−0.447
e	The S is at the top of the surface O	−0.058	2.398	1.490	1.502	−0.143
f	The S is at the top of the surface Mg	−0.055	2.373	1.490	1.500	−0.143
g	The S is at the surface bridge	−0.116	2.326	1.508	1.508	−0.202
h	S vacancy on the surface	−0.032	2.984	1.490	1.497	−0.130

As seen in Figure 7 and Table 2, when SO_2 molecules are adsorbed on the MgO (100) surface with adsorption configurations a, c, and d, the adsorption energies are −0.238 eV, −0.239 eV, and −0.239 eV, respectively, and the distances between the adsorbed SO_2 molecules and the surface are 1.855 Å, 1.837 Å, and 1.837 Å, respectively. Further, the charges transferred from the MgO (100) surface to the adsorbed SO_2 molecules after adsorption are 0.440 *e*, 0.448 *e*, and 0.447 *e*, respectively. As shown in Figure 7 and Table 2, compared with configurations a, c, and d, when other adsorption configurations b, e, f, g, and h are adsorbed on the surface of MgO (100), the adsorption energy is smaller, and the adsorption energies are −0.047 eV, −0.058 eV, −0.55 eV, −0.116 eV, and −0.032 eV, respectively. The distances between the adsorbed SO_2 molecules and the surface are large, 2.961 Å, 2.398 Å, 2.373 Å, 2.326 Å, and 2.984 Å, respectively. After adsorption, the charge transferred from MgO (100) surface to the adsorbed SO_2 molecule is small, 0.077 *e*, 0.143 *e*,

0.143 *e*, 0.202 *e*, and 0.130 *e*, respectively [27]. Regarding adsorption energy, geometry, and charge transfer, SO_2 formed strong chemical adsorption with its S-terminal at the oxygen top site, bridge site, and vacancy adsorption of MgO (100). When SO_2 is adsorbed at the surface Mg site at its S end or its O end on the MgO (100) surface, its interaction with the surface is also weak. In addition, by comparing the adsorption energy, structure parameters, and charge transfer of N_2O on the MgO (100) surface, it was found that the interaction between SO_2 and the MgO (100) surface is much stronger than that between N_2O and the surface. The oxygen site on the surface of MgO (100) is the common active site for SO_2 adsorption and N_2O decomposition. However, because of the strong interaction between the SO_2 gas molecules and the surface, the existence of SO_2 will hinder the catalytic decomposition of N_2O on the MgO (100) surface.

When CO exists, it reduces N_2O molecules in the flue gas homogeneously and affects the catalytic decomposition process of N_2O on the surface of MgO (100) [28]. As shown in Figure 8, N_2O molecules will form an adsorbed atomic oxygen on the surface of MgO (100) after oxygen transfer. Thus, if there is only N_2O in the gas atmosphere, the activation energies of the surface reduction according to the LH and ER mechanisms are 0.840 eV and 1.498 eV, respectively. In the presence of CO, the reaction energy diagram of the surface-adsorbed atomic oxygen is shown in Figure 8, wherein the activation energy of the whole reaction process is only 0.086 eV, with 3.934 eV released. Therefore, the existence of CO can improve the rate of surface reduction, but the catalytic activity of the MgO (100) surface for N_2O decomposition is determined by the transfer process of oxygen atoms. Thus, the existence of CO will not improve the catalytic activity of the MgO (100) surface. When comparing the homogeneous reduction of N_2O via CO and the heterogeneous reduction of CO under the catalysis of MgO (100), we found that the heterogeneous reduction of N_2O by CO is a two-step reaction. First, the N_2O molecule undergoes the transfer process of oxygen atoms and must cross the energy barrier of 1.601 eV. Then, the surface reduction process occurs, which requires energy of 0.086 eV. Therefore, the total energy barrier of the catalytic reduction of N_2O by CO on the MgO (100) surface is 1.601 eV, which is slightly lower than that of homogeneous reduction of N_2O by CO (1.691 eV) [18]. Therefore, the reaction rate of CO with N_2O can be increased with the MgO (100) surface.

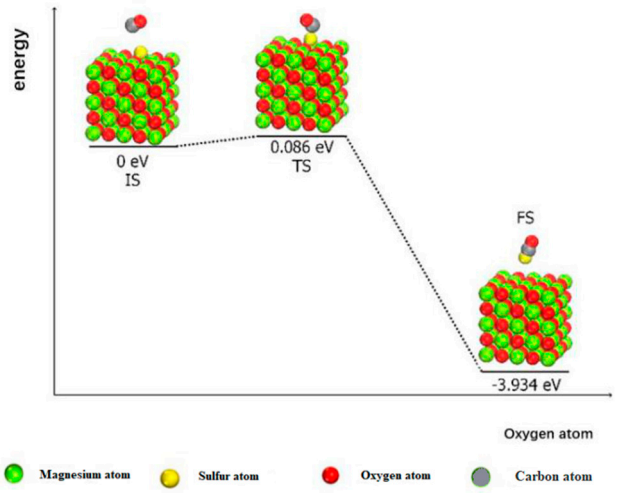

Figure 8. Energy line diagram of MgO (100) surface reduced by CO.

4. Conclusions

In this study, a quantum chemistry method based on the DFT was used to study the decomposition mechanism of N_2O on a MgO (100) surface and the effect of SO_2 and CO on the catalytic N_2O decomposition on the MgO (100) surface. The decomposition of N_2O on the MgO (100) surface is a two-step reaction consisting of oxygen atom transfer and surface reduction. The activation energy of the oxygen transfer process is 1.601 eV, and

the surface reduction process can be carried out according to the ER or LH mechanisms, wherein its activation energies are 1.502 eV and 0.840 eV, respectively. By comparing the corresponding energy change process of ER mechanism and the LH mechanism, it can be concluded that the corresponding path of the LH mechanism is more likely to react. According to the adsorption of N_2O molecules on the surface and the desorption of N_2 and O_2, the reaction energy barrier of N_2O decomposition in MgO (100) is 1.601 eV, and its constant rate step is the transfer process of oxygen atoms, and its catalytic performance for N_2O decomposition is weaker than that of the CaO (100) and CaS (100) surfaces. In addition, by comparing the adsorption energy, structure parameters, and charge transfer of N_2O on the MgO (100) surface in Figures 3 and 7 and Tables 1 and 2, we can see that the adsorption energy, structure parameters, and charge transfer of N_2O on the surface of N_2O, the presence of SO_2 competes with N_2O for the active oxygen sites on the surface of MgO (100), thus reducing the catalytic activity of MgO (100). However, CO can accelerate the reduction of the MgO (100) surface and, compared with the homogeneous reaction; the MgO (100) surface can catalyze the reduction of N_2O by CO to a limited extent (wherein the activation energy decreases from 1.691 eV to 1.601 eV (According to the previous research, the barrier of homogeneous reduction of N_2O by CO was determined from the energy distribution diagram [18]).

Author Contributions: Conceptualization, X.H.; Investigation, X.H., W.L. and L.W.; Writing—Original Draft, E.Z.; Writing—Review & Editing, E.Z., Y.Z. and H.Z.; Methodology, X.H., W.L. and L.W.; Validation, C.D. and H.Z.; Guidance, X.H. and C.D. All authors have read and agreed to the published version of the manuscript.

Funding: We are thankful for the support of the National Natural Science Foundation of China (grant number 51776070) and the Special Fund for Basic Scientific Research Expenses of the Central University (grant number 2018 ZD08).

Institutional Review Board Statement: Not applicable.

Informed Consent Statement: Not applicable.

Data Availability Statement: The data presented in this study are available upon request from the corresponding author.

Conflicts of Interest: The authors declare that they have no known competing financial interests or personal relationships that could have appeared to influence the work reported in this paper.

References

1. *GB13223-2011*; Emission Standard of Air Pollutants for Thermal Power Plants. The Ministry of Environmental Protection; The State Administration of Quality Supervision: Beijing, China, 2011.
2. Bonn, B.; Pelz, G.; Baumann, H. Formation and decomposition of N_2O in fluidized bed boilers. *Fuel* **1995**, *74*, 165–171. [CrossRef]
3. United States Environmental Protection Agency. Overview of Greenhouse Gases [OL]. [31 March 2015]. Available online: http://epa.gov/climatechange/ghgemissions/gases/n2o.html (accessed on 11 January 2022.).
4. Ravishankara, A.R.; Daniel, J.S.; Portmann, R.W. Nitrous oxide (N_2O): The dominant ozone-depleting substance emitted in the 21st century. *Science* **2009**, *326*, 123–125. [CrossRef] [PubMed]
5. Haul, R.A.W.; Markus, J. On the thermal decomposition of dolomite. IV. thermogravimetric investigation of the dolomite decomposition. *J. Appl. Chem.* **1952**, *2*, 298–306. [CrossRef]
6. Xu, Y.; Li, J.; Zhang, Y. Conversion of N_2O to N_2 on MgO (001) surface with vacancy: A DFT study. *Chin. J. Chem.* **2003**, *21*, 1123–1129. [CrossRef]
7. Snis, A.; Miettinen, H. Catalytic decomposition of N_2O on CaO and MgO: Experiments and ab initio calculations. *J. Phys. Chem. B* **1998**, *102*, 2555–2561. [CrossRef]
8. Piskorz, W.; Zasada, F.; Stelmachowski, P.; Diwald, O.; Kotarba, A.; Sojka, Z. Computational and Experimental Investigations into N_2O Decomposition over MgO Nanocrystals from Thorough Molecular Mechanism to ab initio Microkinetics. *J. Phys. Chem. C* **2011**, *115*, 22451–22460. [CrossRef]
9. Esrafili, M.D.; Saeidi, N. Carbon-doped boron nitride nanosheet as a promising catalyst for N_2O reduction by CO or SO_2 molecule: A comparative DFT study. *Appl. Surf. Sci.* **2018**, *444*, 584–589. [CrossRef]
10. Esrafili, M. Single Si atom supported on defective boron nitride nanosheet as a promising metal-free catalyst for N_2O reduction by CO or SO_2 molecule: A computational study. *Int. J. Quantum Chem.* **2018**, *118*, e25646. [CrossRef]

11. Chen, P.; Gu, M.; Chen, G.; Liu, F.; Lin, Y. DFT study on the reaction mechanism of N_2O reduction with CO catalyzed by char. *Fuel* **2019**, *254*, 115666. [CrossRef]
12. Esrafili, M.; Heydari, S. Carbon-doped boron-nitride fullerenes as efficient metal-free catalysts for oxidation of SO_2: A DFT study. *Struct. Chem.* **2017**, *29*, 275–283. [CrossRef]
13. Delley, B. An all-electron numerical method for solving the local density functional for polyatomic molecules. *J. Chem. Phys.* **1990**, *92*, 508–517. [CrossRef]
14. Delley, B. From molecules to solids with the $DMol^3$ approach. *J. Chem. Phys.* **2000**, *113*, 7756–7764. [CrossRef]
15. Perdew, J.P.; Burke, K.; Ernzerhof, M. Generalized Gradient Approximation Made Simple. *Phys. Rev. Lett.* **1996**, *77*, 3865–3868. [CrossRef] [PubMed]
16. Inada, Y.; Orita, H. Efficiency of numerical basis sets for predicting the binding energies of hydrogen bonded complexes: Evidence of small basis set superposition error compared to Gaussian basis sets. *J. Comput. Chem.* **2008**, *29*, 225–232. [CrossRef]
17. Wu, L.; Qin, W.; Hu, X.; Dong, C.; Yang, Y. Mechanism study on the influence of in situ SO_x removal on N_2O emission in CFB boiler. *Appl. Surf. Sci.* **2015**, *333*, 194–200. [CrossRef]
18. Wu, L.; Qin, W.; Hu, X.; Ju, S.; Dong, C.; Yang, Y. Decomposition and reduction of N_2O on CaS (100) surface: A theoretical account. *Surf. Sci.* **2015**, *632*, 83–87. [CrossRef]
19. Piskorz, W.; Zasada, F.; Stelmachowski, P.; Kotarba, A.; Sojka, Z. DFT modeling of reaction mechanism and ab initio microkinetics of catalytic N_2O decomposition over alkaline earth oxides: From molecular orbital picture account to simulation of transient and stationary rate profiles. *J. Phys. Chem. C* **2013**, *117*, 18488–18501. [CrossRef]
20. Monkhorst, H.; Pack, J. Special points for Brillouin-zone integrations. *Phys. Rev. B* **1976**, *13*, 5188–5192. [CrossRef]
21. Govind, N.; Petersen, M.; Fitzgerald, G.; King-Smith, D.; Andzelm, J. A generalized synchronous transit method for transition state location. Comp. *Mater. Sci.* **2003**, *28*, 250–258.
22. Lazar, P.; Otyepka, M. Accurate surface energies from first principles. *Phys. Rev. B* **2015**, *91*, 115402. [CrossRef]
23. Chen, P.; Huang, Y.; Shi, Z.; Chen, X.; Li, N. Improving the Catalytic CO_2 Reduction on $Cs_2AgBiBr_6$ by Halide Defect Engineering: A DFT Study. *Materials* **2021**, *14*, 2469. [CrossRef] [PubMed]
24. Cheng, J.; Wang, P.; Hua, C.; Yang, Y.; Zhang, Z. The Impact of Iron Adsorption on the Electronic and Photocatalytic Properties of the Zinc Oxide (0001) Surface: A First-Principles Study. *Materials* **2018**, *11*, 417. [CrossRef] [PubMed]
25. Broqvist, P.; Grönbeck, H.; Panas, I. Surface properties of alkaline earth metal oxides. *Surf. Sci.* **2004**, *554*, 262–271. [CrossRef]
26. Karlsen, E.J.; Nygren, M.A.; Pettersson, L.G.M. Theoretical study on the decomposition of N_2O over alkaline earth metal-oxides: MgO−BaO. *J. Phys. Chem. A* **2002**, *106*, 7868–7875. [CrossRef]
27. Wang, M.; Chen, Y.; Wang, W.; Zhang, T. Adsorption of SO_2 on pristine and defective single-walled MgO nanotubes: A dispersion-corrected density-functional theory (DFT-D) study. *Mater. Res. Express* **2021**, *8*, 015023. [CrossRef]
28. Hu, X.; Dong, C.; Yang, Y.; Qin, W. Experimental and Mechanism Study of Homogeneous N_2O Decomposition with Biomass Gasification Gas and Its Components. *Energy Sources Part A Recovery Util. Environ. Eff.* **2015**, *37*, 11–18. [CrossRef]